International Journal of Scientific Research in Chemical Sciences **Research Paper**
Vol.6, Issue.1, pp.1-9, Feb (2019) **E-ISSN:** 2455-3174
DOI: https://doi.org/10.26438/ijsrcs/v6i1.1-9

Enhanced antimicrobial activity of Zinc oxide nanoparticles with controled particle size by current density.

M.A. Al-Hubaishi[1], S. Gaikwad[2], A.S. Rajbhoj[3*]

Dept. Chemistry, Dr.Bababsaheb Ambedkar Marthwada University, Aurangabad, India

[*]Corresponding Author: anjali.rajbhoj@gmail.com, Tel.: +00-91-9423352320

Available online at: www.isroset.org

Received: 11/Jan/2019, Accepted: 08/Feb/2019, Online: 28/Feb/2019

Abstract— In this study, it was found that by using electrochemical reduction method, the current density have played important role in controlling size and shape of ZnO nanoparticles. Where it were synthesized at 9 and 18 mA /cm2. The results of charaterization indicated metallic nature and absorption peak in the UV region. FTIR and EDX confirmed formation of ZnO and removing of capping agent after calcination , XRD, FESEM and HRTEM showed that size of ZnO nanoflower and nanosheets to be 46.54 nm and 37.3 nm at 9 and 18 mA /cm2 respectively. ZnO NPs is pure and polycrystalline with a hexagonal wurtzite phase. The in vitro antibacterial properties of two synthesized ZnO NPs against two types of bacteria; Gram-postive(staphylococcus aureus) and Gram-negtive(xanthomonas) were examined by diffusion method. It was noticed that the smallest-sized ZnO NPs demonstrated a better antibacterial activity against both bacterial strains as compared to the larger ZnO NPs, the inhibitory effect of ZnO NPs increased with the increase in concentration of ZnO NPs.

Keywords— *electrochemical reduction method, current density, ZnO NPs, particle size, Tetrabutyl ammonium bromide, antimicrobalactivity.*

I. INTRODUCTION

Nanoscience and nanotechnology seek to obtain materials with better, wider, and more useful applications by obtaining very small size on nanometer scale. The size of particulate materials play an important role in determining magnetic, electrical, optical, and other properties and therefore received increased attention in control of the particles size [1]. Various studies on synthesis of nanomaterials of different sizes and effect of size on their properties and applications have been studied [2-4]. Electrochemical reduction method is one of most important and easier methods to prepare metal oxide nanoparticles, which is achieved by passing an electric current between electrodes separated by electrolyte. Reetz and Helbig developed this method in 1994 to size-selective synthesis of nanostructured transition metal clusters in non- aqueous medium [5], and many researchers have used this method for synthesis nanoparticles with different size by controlling current density or capping agent.

In recent years, metallic oxide nanoparticles, specifically ZnO have gained considerable importance due to their unique electronic, optical, mechanical, magnetic and chemical properties that are significantly different from those of bulk counterpart [6-8] and their wide range of applications in various fields of science, in UV- absorbers[9], gas sensors [10], photocatalytic activity [11], antimicrobial activity [12,13], biomedical [14], and water disinfection [15]. Several physical and chemical methods have been developed to obtain ZnO NPs with different morphology and size such as Precipitation [16-18], solvothermal [19, 20] and sol-gel [21, 22].

In recent years, metallic oxide nanoparticles, specifically ZnO have gained considerable importance due to their unique electronic, optical, mechanical, magnetic and chemical properties that are significantly different from those of bulk counterpart [6-8] and their wide range of applications in various fields of science, in UV- absorbers[9], gas sensors [10], photocatalytic activity [11], antimicrobial activity [12,13], biomedical [14], and water disinfection [15]. Several physical and chemical methods have been developed to obtain ZnO NPs with different morphology and size such as Precipitation [16-18], solvothermal [19, 20] and sol-gel [21, 22]. In this study, we successfully synthesized ZnO NPs with different size and shapes by adjusting current density via electrochemical reduction method. It was studied size and shape of particles by FESEM, XRD and HRTEM. We investigated the antibacterial activities of ZnO nanoparticle with different sizes against two important opportunistic positive gram and negative gram Staphylococcus *aureus* and *Xanthomonas* respectively which

known to be resistant to many of antibacterial agents. We found that particle size decrease with increasing current density. The smallest size of particle is more effective than bigger.

II. MATERIALS AND CHEMICALS

Zinc (Zn) and platinum (Pt) sheets (99.99) having thickness 0.25 mm were purchased from Alfa Aesar, tetrabutylammonium bromide (TBAB) and distilled water.

III. METHODOLOGY

synthesis of ZnO nanoparticles

ZnO NPs were synthesized by electrochemical method in an undivided two electrodes cell, consisting of pure Zn metal foil (scrificial anode) and Pt foil (cathode). Before the experment, Pt and Zn electrodes were cleaned by emery paper and then dilute HCl . Both electrodes were washed thoroughly with distilled water. Electrolytic medium was prepared by dissolving TBAB (0.01 M) in distilled water. TBAB served as both stabilizing agent as well as supporting electrolyte. During all experments, a constant distance of 1 cm was maintained between two electrodes with continuos stirring and constant current density of 9 or 18 mA/cm^2 was applied for 2 h.

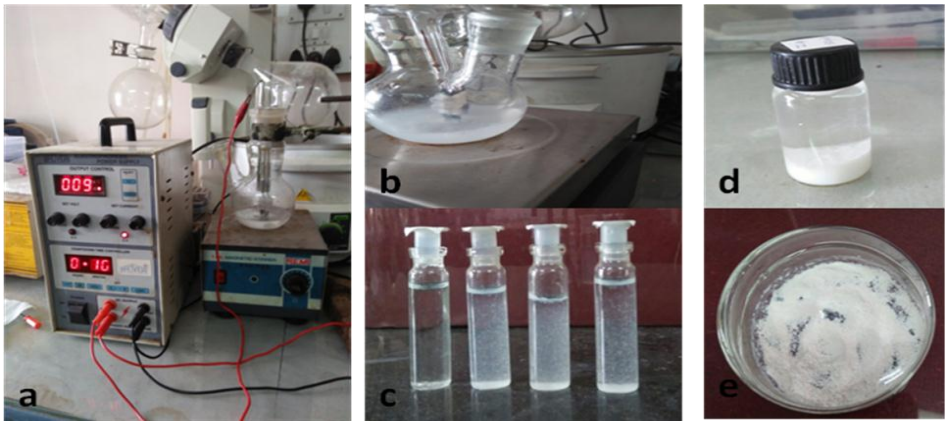

Figure 1. (a) Electrophoresis setup for synthesis metal oxide NPs, (b) ZnO NPS formed in action, (c) ZnO NPs after 30, 60, 90 and 120 min of reaction, (d) after settle and washing, (e) after drying.

The experimental set up is shown in fig.1, dissolution of zinc electrode was observed upon applying current. This results in the formation of Zn^{2+} ions which get oxidized by atmospheric oxygen forming of ZnO nanoclusters, which were stabilized by TBAB. Initial clear solution becomes turbid after some time which indicates formation of ZnO NPs. Amount of turbidity goes on increasing with time. White ZnO NPs were allowed to settle for 3 h. the solid sample was separated from the solution by decantation and washed 2-3 times with distilled water to remove exces of TBAB then dried in a vacuum desiccator at room temperture for 24 h and calcinated at 500 C for 2 h and used for charaterization and application. Effect of current desity on size ZnO NPs was studied by performing experiments in different current density such as at 9 and 18 mA/cm^2. Samples prepared at 9 and 18 mA/cm^2 were labeled as Z-9 and Z-18 respectively.

Characterization of ZnO NPs

The prepared ZnO NPs were characterized by UV- Vis spectrophotometer (UV -1800 Shimadzu) using a quartz cuvette with distilled water as a reference. Fourier transform infrared spectroscopy (FT-IR) was used to study the interaction of ZnO NPs with TBAB. FT-IR of powder samples was acquired on (FT-IR, Shimadzu,) spectrometer in the range of 400-4000 cm-1. To determine phase purity and crystal structure powder, X- ray diffraction (XRD) study was done on X-ray powder diffratometer (PW3050), operating at 20 kv. The diffractogram was recorded in the range of (2θ°) 10° to 90° using Cu-Kα radiation (λ= 1.5406 A°). The average crystalline size (d) was estimated using the Debye Scherrer equation. Morphology structures were investigated by Field Emission Scanning Electron Microscopy (FESEM) on Hitachi-PU 5.0KV 8.3mm *120k SE(UL). High Resolution transmission electron microscopy (HRTEM) study was carried out on JEOL Model /JEM - 2100, Resolution(Point: 0.23nm, Lattice: 0.14 nm), Voltage(200kV).

Antibacterial Activity

The effect of prepared ZnO NPs have been tested against two types of bacteria; Gram-postive(Staphylococcus Aureus) and Gram-negtive(Xanthomonas) by diffusion method, for four different concentrations of ZnO NPs i.e. 40µl,80µl,120µl,160µl and compared with well known antibiotic Streptomycin.

IV. Results and Discussion

Optical study

The metal NPs exhibit board absorption bands in the UV-Visible range due to the excitation of surface Plasmon resonance (SPR), these SPR are characteristic prosperities for the metallic nature of particles. The UV-Visible spectra recorded for synthesized NPs after various times 30, 60, 90 and after complete electrolysis process 120 min, as shown in fig.2.a, b UV-Vis absorbance spectrum shows that a characteristic band 281 nm and 278 nm for Z-9 and Z-18 respectively. The intensity of the characteristic band increased with time which indicated the formation of ZnO NPs.

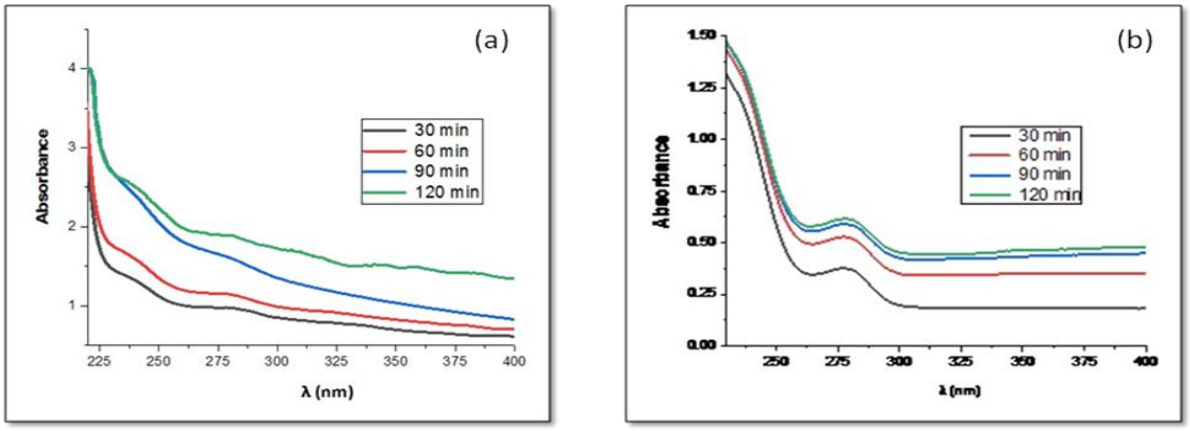

Figure 2. UV-Vis of ZnO NPs after 30, 60, 90 and 120 min of reaction (a) Z-9, (b) Z-18.

FT-IR study

The interaction of stabilizer (TBAB) with ZnO NPs was studied by FTIR spectroscopy, fig.3. (a, b) depict the FTIR spectra of TBAB stabilized samples of ZnO NPs before and after calcinations.

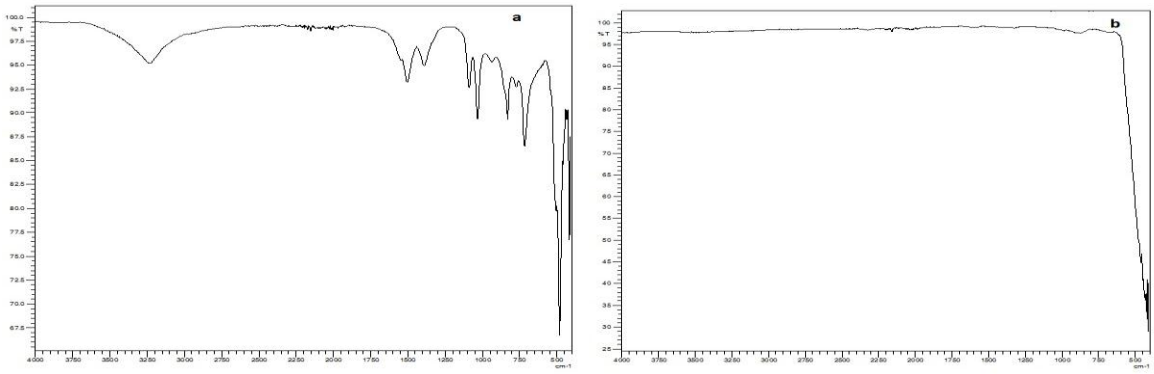

Figure 3. FTIR spectra of sample (a) before and (b) after calcination.

The interaction of stabilizer (TBAB) with ZnO NS was studied by FTIR spectroscopy, Fig.2. (b) depict the FTIR spectra of TBAB stabilized samples of ZnO NS before and after calcinations. The FTIR spectra of sample before calcinations show broad peak at 3226, 1031, 1087 and 717 cm-1 is assigned to stretching vibration of TBAB. Only the strong absorption between 420 and 464cm-1 remained corresponding to Zn-O stretching which are attributed to the formation of zinc oxide NPs which are almost free from any organic impurity.

X-Ray Diffraction Study

Fig.4. show the XRD pattern of ZnO NPs with diffraction peaks at 31.18, 34.44, 36.26, 47.55, 56.60, 62.87, 67.96 which correspond to the lattice planes (100), (002), (101), (102), (110), (103), (112) respectively, with lattice parameter a= 3.249, b= 3.249, c= 5.206, α = β = 90, ϒ= 120 of the hexagonal Wurtzite phase of ZnO NPs (JCPDF file card no. 36-1454). The high crystalline and purity of ZnO NPs were confirmed by the absence of any impurity peaks. The average crystallite size of ZnO NPs determined from X-ray line broadening measurement using the Debye-Scherer equation (**d= kλ / βcosθ**) was found to be 46.54 nm and 37.3 nm for Z-9 and Z-18 respectively. Where d the crystalline size, β denotes the full width at half maximum of high intense diffraction peak, diffraction angle is denoted by θ and the wavelength of X-ray is denoted by λ.

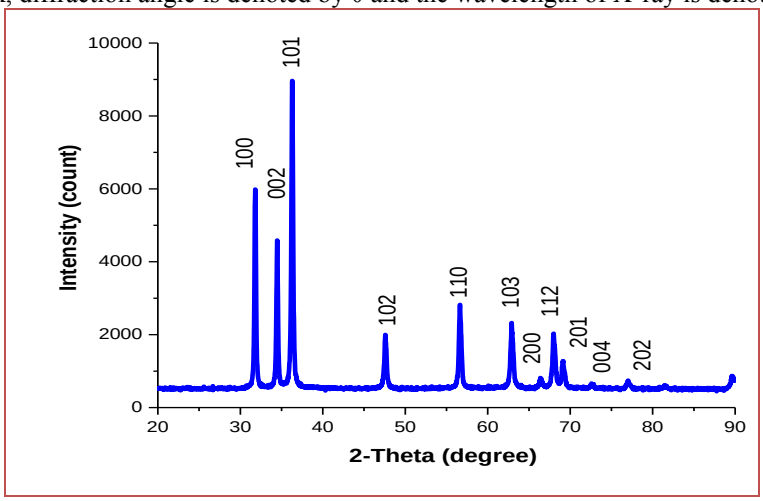

Figure 4. XRD pattern of ZnO NPs.

XRD plot show the intense peaks of TBAB at different current density 9 and 18 mA/cm^2 for (101) plane the full width of half maximum (FWHM) value increases with decreasing the particle size as shown in the table1.

Table1. The effect of current density on size of ZnO NPs

ZnO NPs	2θ°	hkl	FWHM	Crystalline Size (nm)
Z-9	**36.2604°**	**101**	**0.1629**	**51.31**
Z-18	**36.2654°**	**101**	**0.1865**	**44..19**

Morphological Study

FESEM imaging technique was utilized to acquire information about the particle morphology in nanoscale. Fig.5.a,b show the SEM images of Z-9 and Z-18 like flower and sheets shapes respectively. The results indicate that highly crystalline ZnO NPs were obtained.

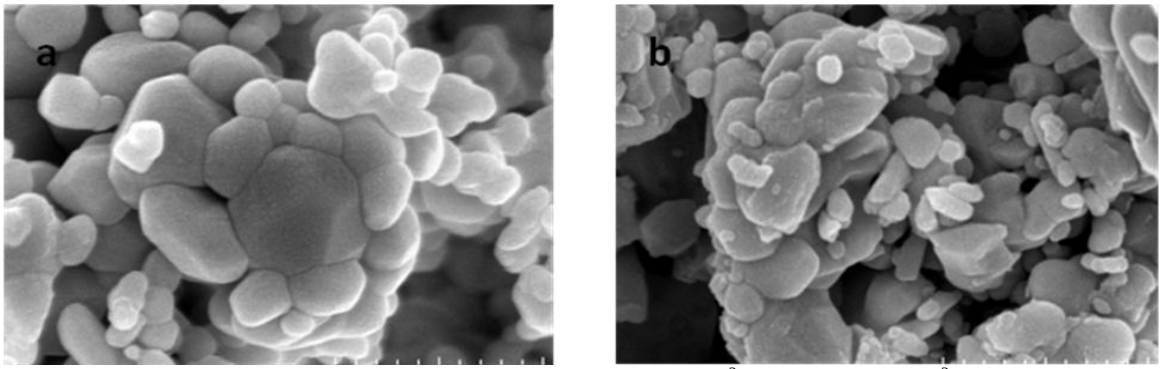

Figure 5. FESEM images of ZnO NPs (a) at 9 mA/cm^2 and (b) at 18 mA/cm^2

Composition of ZnO NPs (EDX)

The chemical composition of the samples was examined using EDX (Energy Dispersive X-ray spectroscopy) in fig.6. Quantitative measuring results obtained from EDX analysis reflect the purity of ZnO NPs. The EDX measurements indicate the presence of Zn along with O peaks.

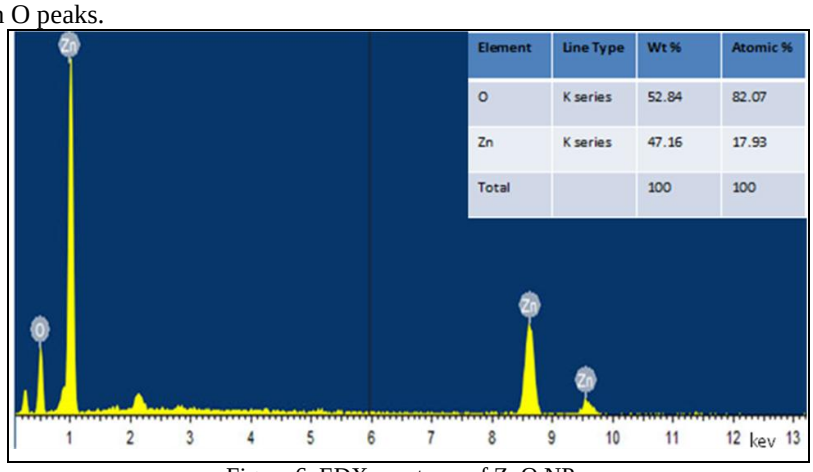

Figure 6 EDX spectrum of ZnO NPs.

Size and crystallite HRTEM and SAED

Effect of current density on particle size by this method was further confirmed by HRTEM analysis. Micrographs indicate that most particles were fine with various sizes, spherical, elongated and some clusters have also been observed. The average particles diameter measured was 52 – 92 nm and 23 – 46 nm with different current densities at 9 mA/cm^2 and 18 mA/cm^2 respectively, these results clearly indicate the decrease in particles size with increase in current density, which resemble to the phenomenon observed in XRD pattern. The lattice fringes are also visible, the distance between two lattice fringes was observed to be 0.18 nm and which corresponds to the (102) reflection of Z -9 fig.7 (c), and 0.25 nm which corresponds to the (101) reflection of Z -18 fig.8 (c) .SAED pattern shown in fig.8(d) indicates that the polycrystalline nature of the electrochemically synthesized ZnO NPs , for which five ring patterns with plane (100), (002), (101), (102) and (110) of ZnO NPs at both current densities.

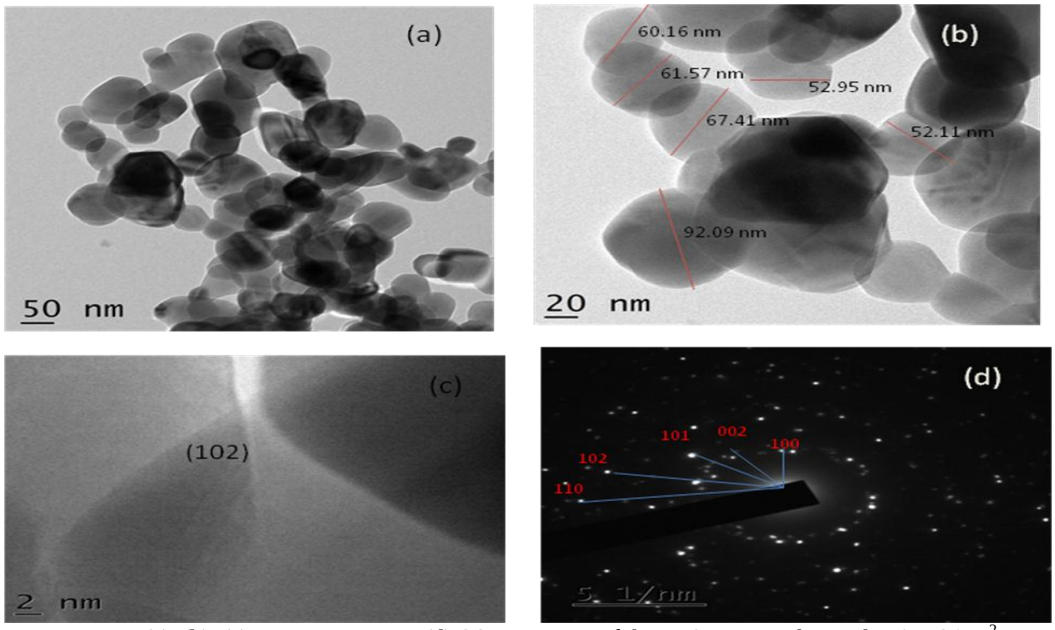

Figure 7. (a), (b), (c) HRTEM images, (d) SAED pattern of the ZnO NPs synthesized at 9 mA/cm^2.

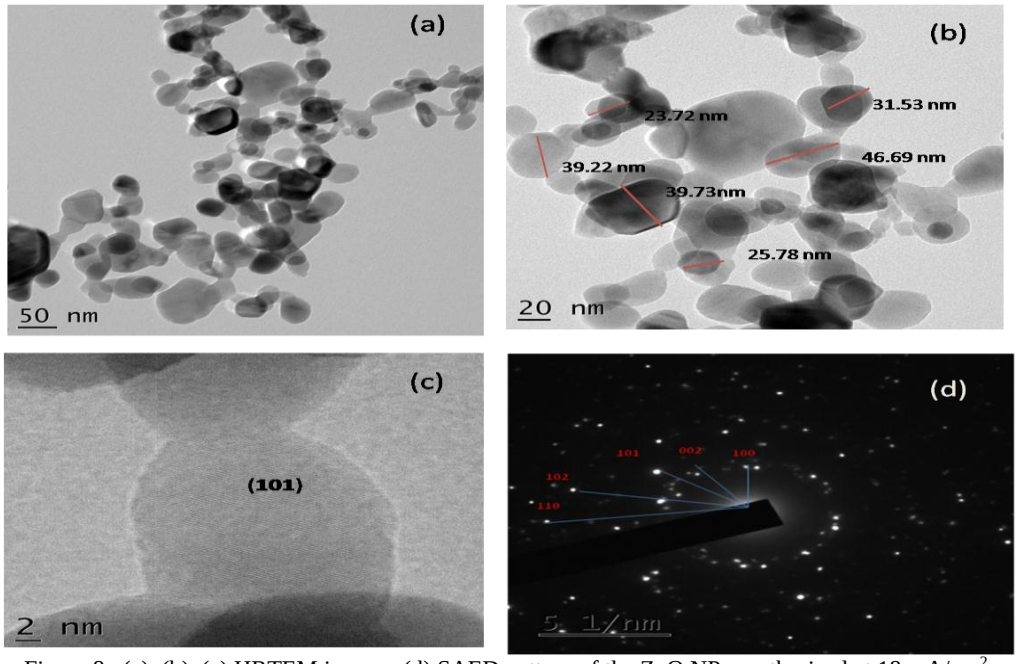

Figure 8. (a), (b), (c) HRTEM images, (d) SAED pattern of the ZnO NPs synthesized at 18 mA/cm^2.

Antibacterial Activity of ZnO NPs

The antibacterial activity of ZnO NPs was tested against two bacterial strains positive gram and negative gram *Staphylococcus aureus* and *Xanthomonas* respectively. Table 2. and fig. 9-11 represent the antibacterial activity of ZnO NPs different sizes for positive and negative gram in a well diffusion technique.

Table2. antibacterial results of ZnO NPs with different sizes, different concentrations and different microorganisms.

	Diameters of microbial growth inhibition zone (nm)							
	Xanthomonas (-)				S. Aureus (+)			
Quantity (µl)	**40**	**80**	**120**	**160**	**40**	**80**	**120**	**160**
DMSO	0	0	0	0	0	0	0	0
Z-9	0	0	13	16	0	0	12	16
Z-18	0	16	17	18	0	12	15	17
Streptomycin	30	33	34	35	31	33	35	36

The results indicated that ZnO NPs synthesized by electrochemical reduction method showed effective antibacterial activity against pathogenic bacteria. The results showed that the inhibitory effect of ZnO NPs increased with the decrease in particle size and increased with the increase in concentration. The DMSO control did not show any antibacterial activity against the tested bacterial strains.

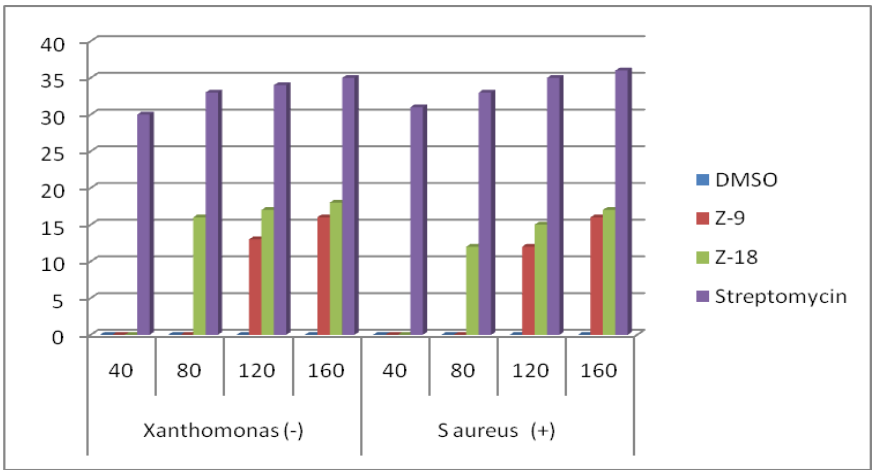

Figure 9. Zone of inhibition in (mm) of ZnO NPs with different sizes, different concentrations and different microorganisms.

Figure 10. Zone of inhibition formed against Xanthomonas

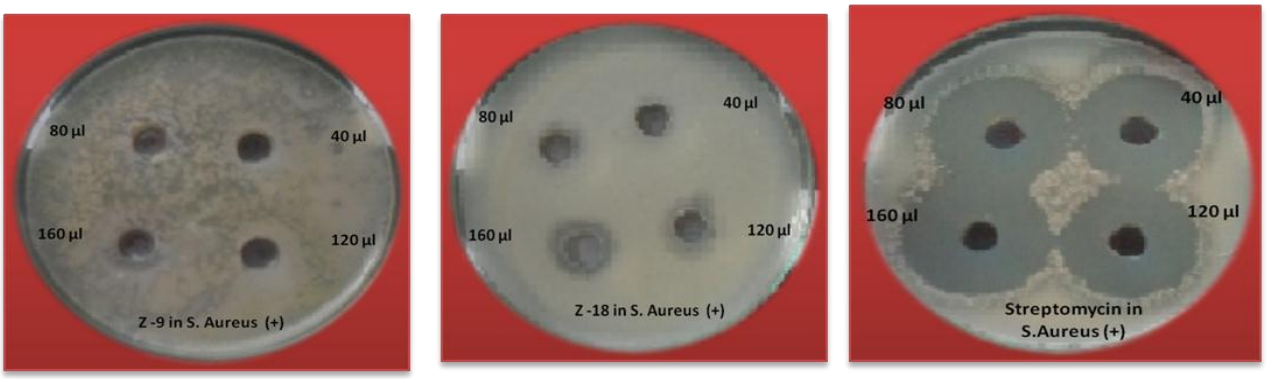

Figure 11. zone of inhibition formed against S. Aureus.

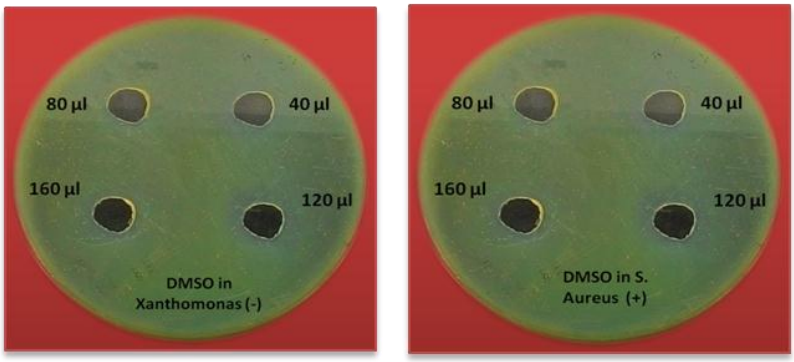

Figure 12. zone of inhibition formed of control (DMSO) against Xanthomonas and S.Aureus.

V. CONCLUSION AND FUTURE SCOPE

ZnO NPs of different sizes successfully synthesized by electrochemical reduction method, and the current density is very good to control nanoparticle size. The results showed that ZnO is in nanometer scale 46.54 nm and 37.3 nm for Z-9 and Z-18 respectively, pure and polycrystalline with a hexagonal wurtzite phase of both sizes ZnO. The particle size decrease with increasing current density, inhibitory effect of ZnO NPs against pathogenic bacteria increased with the decrease in particle size and increased with the increase in concentration.

ACKNOWLEDGMENT *(HEADING 5)*

The authors are grateful to the DST-FBT and WGC-SAP for their financial support, STIC Cochin for HRTEM analysis and SAIF Punjab University for XRD and FESEM analysis.

REFERENCES

[1] Kiss, F. D., Miotto, R., & Ferraz, A. C. (2011). Size effects on silver nanoparticles ’. *Nanotechnology*, *275708*(22), 1–9.
[2] Ajitha, B., Kumar, Y. A., & Reddy, P. S. (2015). Enhanced antimicrobial activity of silver nanoparticles with controlled particle size by pH variation. *Powder Technology*, *269*, 110–117.
[3] Suchomel, P., Kvitek, L., Prucek, R., Panacek, A., Halder, A., Vajda, S., & Zboril, R. (2018). Simple size-controlled synthesis of Au nanoparticles and their size- dependent catalytic activity. *Scientific Reports*, (February), 1–11.
[4] Raza, M. A., Kanwal, Z., Rauf, A., Sabri, A. N., & Riaz, S. (2016). Size- and Shape-Dependent Antibacterial Studies of Silver Nanoparticles Synthesized by Wet Chemical Routes. *Nanomaterials*, *6*(74), 2–15.
[5] Reetz, M. T.; Helbig, W. Size-Selective Synthesis of Nanostructured Transition Metal Clusters. *J. Am. Chem.*SOC, 1994, (1 1), 1401–1402.
[6] Mazur, M. (2004). Electrochemically prepared silver nanoflakes and nanowires. ELECTROCHEM COMMUN, 6, 400–403.
[7] Feng, L., Zhang, C., Gao, G., & Cui, D. (2012). Facile synthesis of hollow Cu 2 O octahedral and spherical nanocrystals and their morphology-dependent photocatalytic properties. Nanoscale Research Letters, 7(4), 1–10.
[8] Lee, C. Y., Li, S. Y., Lin, P., & Tseng, T. Y. (2005). ZnO Nanowires Hydrothermally Grown on PET Polymer Substrates and Their Characteristics. *Journal of Nanoscience and Nanotechnology*, *5*, 1088–1094.
[9] Baglioni, P. (2008). Synthesis and characterization of zinc oxide nanoparticles : application to textiles as UV-absorbers. *Journal of Nanoparticle Research*, *10*(4), 679–689.
[10] Bhatia, S., Verma, N., & Bedi, R. K. (2017). Results in Physics Ethanol gas sensor based upon ZnO nanoparticles prepared by different techniques. *Results in Physics*, *7*, 801–806.
[11] Stan, M., Popa, A., Toloman, D., Dehelean, A., Lung, I., & Katona, G. (2015). Materials Science in Semiconductor Processing Enhanced photocatalytic degradation properties of zinc oxide nanoparticles synthesized by using plant extracts. *Materials Science in Semiconductor Processing*, *39*, 23–29.
[12] Dobrucka, R. (2016). Biosynthesis and antibacterial activity of ZnO nanoparticles using Trifolium pratense flower extract. *Saudi Journal of Biological Sciences*, *23*(4), 517–523.
[13] Gunalan, S., Sivaraj, R., & Rajendran, V. (2013). Progress in Natural Science : Materials International Green synthesized ZnO nanoparticles against bacterial and fungal pathogens. *Progress in Natural Science: Materials International*, *22*(6), 693–700.
[14] Jiang, J., Pi, J., & Cai, J. (2018). The Advancing of Zinc Oxide Nanoparticles for Biomedical Applications. *Hindawi Bioinorganic Chemistry and Applications*, *2018*, 1–18.
[15] Asuncion, E., Dimapilis, S., Hsu, C., Marie, R., Mendoza, O., & Lu, M. (2018). Zinc oxide nanoparticles for water disinfection. *Sustainable Environment Research*, *28*(2), 47–56.
[16]Sharma, R. K., & Ghose, R. (2014). Synthesis of zinc oxide nanoparticles by homogeneous precipitation method and its application in antifungal activity against Candida albicans. *Ceramic International*, *41*(1), 967–975.

[17]Wang, Y., Zhang, C., Bi, S., & Luo, G. (2010). Preparation of ZnO nanoparticles using the direct precipitation method in a membrane dispersion micro-structured reactor. *Powder Technology*, *202*(1–3), 130–136.

[18] Raou, D. (2013). Synthesis and microstructural properties of ZnO nanoparticles prepared by precipitation method. *Renewable Energy*, *50*, 932–937.

[19] Xu, L., Hu, Y., Pelligra, C., Chen, C., Jin, L., Huang, H.,Suib, S. L. (2009). ZnO with Different Morphologies Synthesized by Solvothermal Methods for Enhanced Photocatalytic Activity. *Chem. Mater.*, *21*(13), 2875–2885.

[20] Kusumam, T. V. A., Panakkal, T., Divya, T., & Nikhila, M. P. (2015). Morphology controlled synthesis and photocatalytic activity of zinc oxide nanostructures. Ceramic International, 42(3), 3769–3775.

[21] Ba-abbad, M. M., Amir, A., Kadhum, H., Bakar, A., & Takriff, M. S. (2013). The effect of process parameters on the size of ZnO nanoparticles synthesized via the sol – gel technique. *Journal of Alloys and Compounds*, *550*(15), 63–70.

[22] Zak, A. K., Abrishami, M. E., Majid, W. H. A., Yousefi, R., & Hosseini, S. M. (2011). Effects of annealing temperature on some structural and optical properties of ZnO nanoparticles prepared by a modified sol – gel combustion method. *Ceramic International*, *37*(1), 393–398.

AUTHORS PROFILE

Dr. A.S.Rajbhoj, M.Sc. and Ph.D. physical chemistry. She is currently working as Professor in Department of chemistry Dr.B.A.M.U. Dr. S.Gaikwad, M.Sc. and Ph.D in organic chemistry, He is currently working as Professor and head in Department of chemistry Dr.B.A.M.U. Ms. M.A.Al-Hubaishi, M.Sc. in industrial chemistry, she is currently research student in Department of chemistry, Dr.B.A.M.U.

